ARMY RESEARCH LABORATORY

Parameterized Design of a Supersonic Radome

Michael S.L. Hollis

ARL-TR-2418 APRIL 2001

Celazole® is a registered trademark of Celanese Acetate.
I-DEAS® is a registered trademark of Structural Dynamics Research Corporation.
MACOR® is a registered trademark of Dow Corning.
PEEK™ is a trademark of Victrex.
Pentium® is a registered trademark of Intel Corporation.
Torlon® is a registered trademark of Amoco Performance Products.
Ultem® is a registered trademark of GE Plastics.
Vespel® is a registered trademark of E.I. Dupont de Nemours.
Victrex® is a registered trademark of Victrex PLC Corporation - United Kingdom.

Army Research Laboratory
Aberdeen Proving Ground, MD 21005-5066

ARL-TR-2418 April 2001

Parameterized Design of a Supersonic Radome

Michael S.L. Hollis
Weapons and Materials Research Directorate

Abstract

With the new requirements of the future combat systems (FCS), gun-launched projectiles will most likely be decreasing in diameter and increasing in muzzle velocity. In addition, these projectiles will be carrying entire electronic systems, specifically, global positioning system (GPS)/inertial guidance and terminal homing. These systems will sense during the flight and terminal environments of the projectile and will provide data links (probably two-way telemetry) for system diagnostics and dynamic re-targeting. Most of these sensing elements involve various antennae operating at a variety of frequencies ranging from GPS (1.5 GHz) to millimeter wave seekers (94 GHz) to optical seekers (1 PHz). Because of packaging constraints, these systems are likely to be placed forward on the projectile body. All these antennae require a protective "window" for transmitting and/or receiving signals. Based on the location of these systems, that window is usually described as the projectile radome.

The radome must withstand the cannon launch and ballistic environment. The intense aero-heating of supersonic flight softens polymers, thus reducing the structural integrity. Of course, it is obvious that the radome must perform well electronically across a possible wide band of radio frequencies.

This report studies the use of several (polymer types) materials, which can be machined to create a radome of a desired shape. These polymers, which are either extruded or molded into stock shapes, were chosen based on the dielectric constant (relative to air, between 3 and 4) and thermal and structural properties. A generic radome geometry was selected to perform the thermal and structural analyses. An older yawsonde geometry, which was flight tested, was also analyzed.

In addition to suggesting a quick solution, it is also suggested that a more intensive effort be performed to find higher performance material solutions for the design of radomes for FCS-like projectile launch/flight conditions. The aerothermal, convective, conductive and structural analyses are a skeleton of a study that needs to be performed. Other materials such as ceramics, composites, and other polymers also need to be studied.

ACKNOWLEDGMENTS

The author would like to thank the following people for their expertise and guidance in various areas. Mr. Bernard Guidos of the U.S. Army Research Laboratory (ARL) is acknowledged for his continuing guidance in performing aerothermal analyses. Mr. Guidos also provided technical assistance in the application of the ABRES shape change code (ASCC) on various UNIX computing platforms. Dr. Steve McKnight and Dr. William Spurgeon of ARL are also commended for their expertise in polymers and how the mechanics change with time and temperature. Drs. Jerry LaSalvia and Paramel Patel of ARL are also thanked for their knowledge of ceramics, including MACOR®. Bradford Davis and David Hepner of ARL are acknowledged for processing data from a flight test that occurred in August 1999 at Yuma Proving Ground, Arizona. The flight profile was used to create the verification model for this report. Finally, the author would like to thank Ms. Andie Overfield of DSM[1] Engineering Plastic Products for her technical expertise and knowledge of polymers. She was able to answer technical questions and provide material property data in a timely and professional manner.

[1] not an acronym

INTENTIONALLY LEFT BLANK

Contents

Figures

Tables

1. Introduction

With the new requirements of the future combat systems, gun-launched projectiles will most likely be decreasing in diameter and increasing in muzzle velocity. In addition, these projectiles will be carrying electronic systems for global positioning system (GPS)/inertial guidance and terminal homing. These subsystems will require the projectile to sense the flight and terminal environments and to provide data links (probably two-way telemetry) for system diagnostics and dynamic re-targeting. Most of these "sensing" elements involve various antennae operating at a variety of frequencies. Examples range from GPS (1.5 GHz) to millimeter wave seekers (94 GHz) to optical seekers (1 PHz). Because of packaging constraints, these systems will probably be placed forward on the projectile body. All these antennae require a protective "window" for transmitting and/or receiving signals. Based on the location of these systems, that window is usually described as the projectile radome.

The radome must withstand the cannon launch and ballistic environment. The intense aero-heating of supersonic flight softens polymers, thus reducing the structural integrity. Of course, it is obvious that the radome must perform well electronically across a possible wide band of radio frequencies.

Since telemetry and inertial sensors have become more affordable, a diagnostic fuze can be built, based upon a yawsonde (Hepner et al. 2000) (see Figure 1). Originally configured for artillery projectiles, this device is built in other geometries, depending upon the munition requirement. Even this simple device that uses a telemetry antenna under the radome is being examined for possible melting or softening at high launch velocities. The protective radome has been made of polymers such as nylon and polycarbonate because of the materials' strength and radio frequency (RF) transparency.

This report studies the use of several (polymer types) materials, which can be machined to create a radome of a desired shape. These polymers, which are either extruded or molded into stock shapes, were chosen on the basis of the dielectric constant (relative to air, between 3 and 4) and thermal and structural properties.

A generic radome geometry has been selected to perform the thermal and structural analyses. Various polymers, capable of being machined into the

radome geometry, are studied. An older yawsonde geometry, which was flight tested, will also be analyzed.

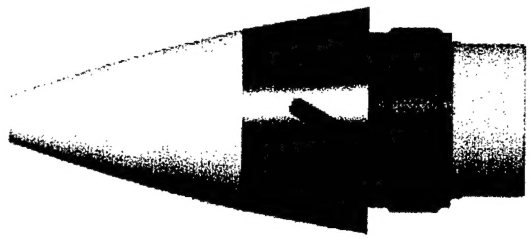

Figure 1. An Example of a Yawsonde.

2. Problem Description

Future gun-launched projectiles will have higher muzzle velocities. There currently exists a need for RF transparent radome solutions with muzzle velocities near Mach numbers equal to 3 (M=3). FCS requirements may push these velocities as high as M=5. Assessments of aerothermal heating requirements for specific radome geometries need to be studied. Trade-off studies involving aerodynamic shape, antenna location, materials, and RF characteristics also need to be made.

This report studies one specific radome geometry and analyzes the aerothermal implications from M=3 to 1.8. Turbulent and laminar boundary conditions are studied in addition to a laminar to turbulent transition scheme. The results from the aerothermal analyses are then entered into a convection-conduction thermal model to determine temperatures throughout the radome geometry. The thermal model is also used to perform linear, quasi-static, finite element structural analyses at launch and at appropriate times in the flight when the computed temperatures reach the polymer softening temperatures.

The final product of this report is twofold. The first is a short-term solution using the extruded/molded plastics to manufacture a radome. The other is a guideline for a more extensive study to find several solutions for high speed, RF transparent radomes for ballistic projectiles.

3. Temperature-Dependent Properties of Polymer Materials

Polymer materials are characterized into two types of plastics: thermoplastics and thermosets. Thermoplastics are broken into two main groups: amorphous and semi-crystalline. Amorphous and semi-crystalline plastics have a glass transition temperature. "Glass transition is a phase change of amorphous solids, such as glasses, metals, and polymers. A non-crystalline material is converted to a relatively hard, elastic and glassy state from a soft, elastic plastic and rubbery state when being cooled through its glass transition temperature Tg" (Li 1999). If Young's Modulus were plotted versus temperature for almost any thermoplastic on a logarithmic scale, then Tg would occur as a step function when the high strength of the polymer changes to a softer state. Thermosets do not have a Tg, but they do soften with temperature.

The materials that were studied in this report are

- Nylon 66, which is unfilled. This semi-crystalline material is very common with a variety of manufacturers.

- Ultem® 1000, an unfilled amorphous polyetherimide, which is manufactured by General Electric Plastics.

- Victrex® polyetheretherketone (PEEK™) 450GL30, which is a general purpose 30% glass fiber-reinforced grade of used for injection molding and extrusion. This semi-crystalline, polymer is manufactured by Victrex®.

- Torlon® 4203L, which is an unfilled polyamideimide semi-crystalline resin, manufactured by British Petroleum (BP) Amoco Chemicals.

- Hoechst Celanese Celazole® polybenzimidazole (PBI), which is an unfilled compression-molded amorphous thermoplastic, manufactured by DSM Engineering Plastics.

- Vespel® SP-1, which is an unfilled high performance polyimide resin, manufactured by DuPont.

- MACOR®, which is a machinable glass ceramic (MGC). This is the only ceramic that was studied. MACOR® has a continuous use temperature of 800° C.

4. In-Flight Surface Heat Transfer

The in-flight (i.e., aerodynamic) heat transfer coefficient distributions were obtained from separate analyses involving the ABRES[1] shape change code (ASCC). ABRES is a computational procedure for predicting the aerodynamic heat environment, shape change, and thermal response of axisymmetrical re-entry bodies (Acurex Corporation 1981). In this report, ASCC was used to predict the computed heat transfer coefficient, h, and the adiabatic wall temperature, T_{aw}, acting along the geometry. ASCC was chosen for the ease of use, speed, and accuracy.

A velocity profile, depicted in Figure 2, is the desired flight profile, for which the heat transfer coefficients are calculated. The flight starts with an M=3 launch and linearly declines to M=1.8 in 4.5 seconds. Figure 3 depicts the hemispherical radome geometry that was used for the analyses.

Figure 4 shows the heat transfer coefficients for the radome at various Mach numbers, and Figure 5 shows T_{aw}. The coefficients were calculated with laminar and turbulent flow conditions. Initially, the convection-conduction thermal model was run with turbulent-only conditions, and the results indicated that the radome, made of Ultem®, would melt very early in the flight. Running the same problem with laminar-only conditions indicated that the same radome would survive. The correct boundary layer case involves a laminar transition; thus, a laminar-turbulent scheme was adapted.

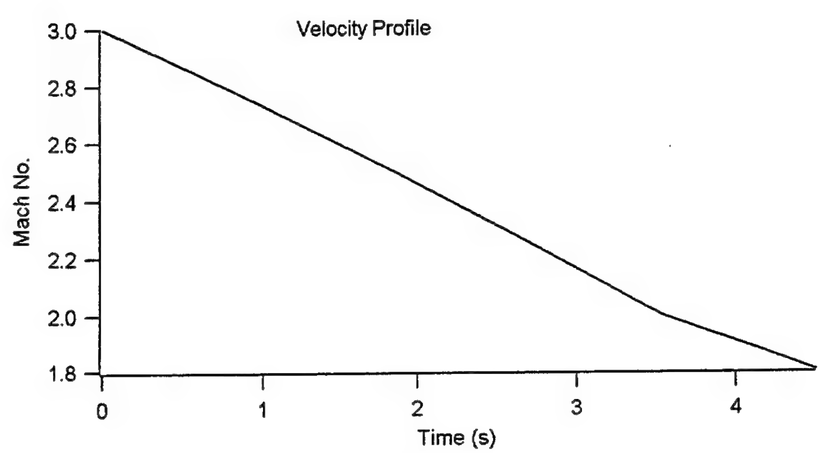

Figure 2. Experimental Velocity Profile.

[1] not an acronym

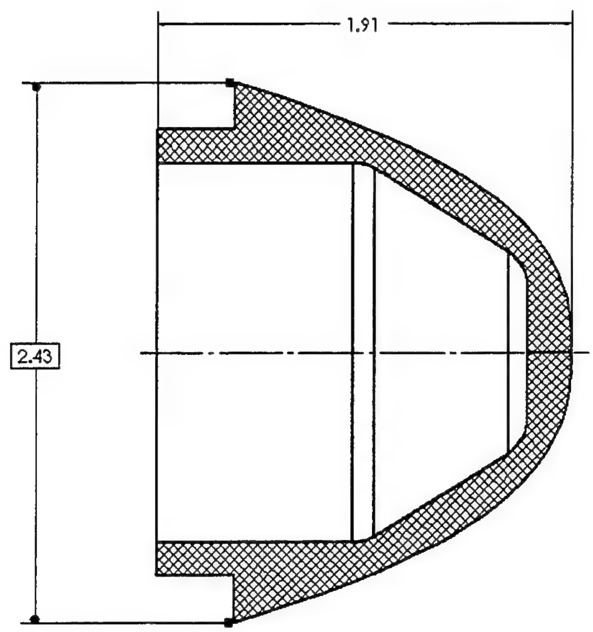

Figure 3. Hemispherical Radome Geometry (units in inches).

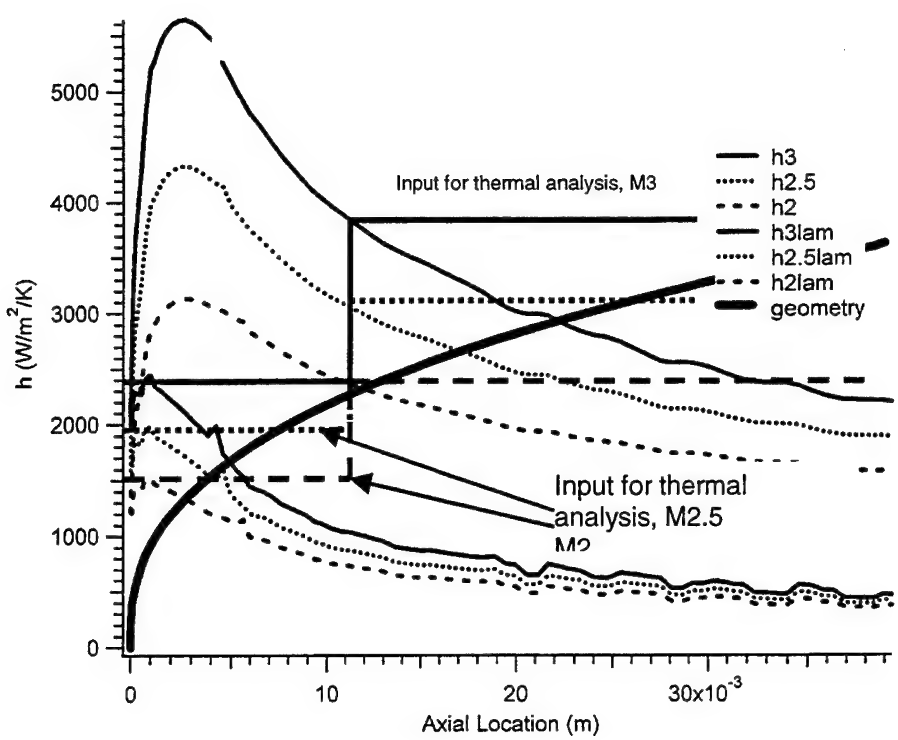

Figure 4. Comparison of Heat Transfer Coefficients at Various Mach Numbers for Turbulent and Laminar Flow Conditions.

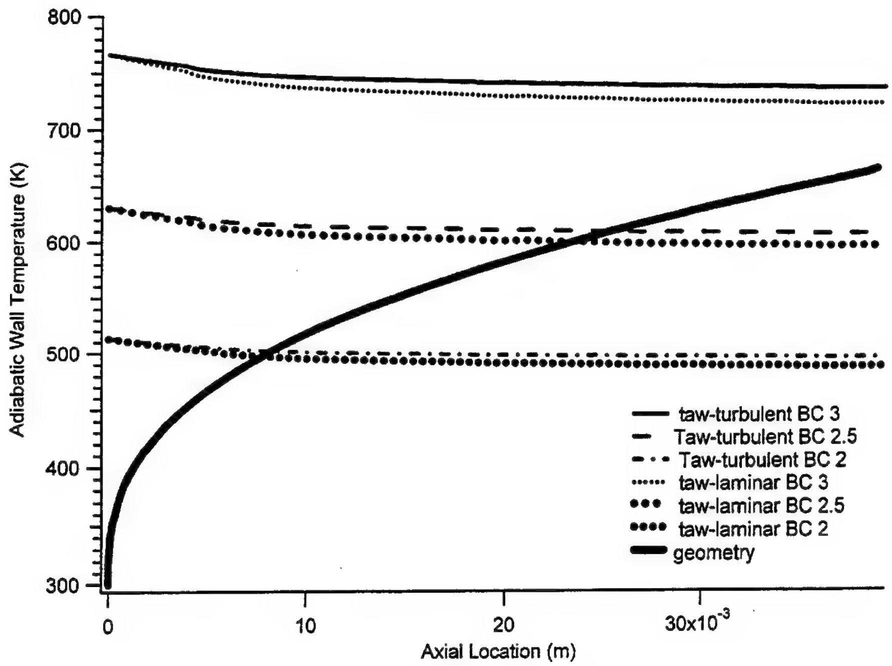

Figure 5. Steady State Adiabatic Wall Temperatures at Various Mach Numbers for Turbulent and Laminar Flow Conditions.

A heat transfer coefficient transition region was imposed in a calculation by Guidos for a nose cap of a 120-mm XM797 (Guidos 1995). Guidos imposed a knurled region on the nose to initiate a transition from laminar flow to turbulent. A similar approach was used for this report. Figure 4 shows the heat transfer coefficients with the transition curves. A linear curve between the laminar curve at 11 mm and the turbulent curve at 21 mm was imposed. However, it was decided to be more conservative and create a step function as depicted in the plot. For instance, for M=3, the initial laminar heat transfer coefficient would be approximately 2500 $W/m^2/K$, with a step transition to a turbulent 3900 $W/m^2/K$ for the rest of the geometry. Heat transfer coefficient and T_{aw} for M=1.8 were calculated via linear interpolation.

4.1 In-depth Thermal Response of the Radome

The author used the same radome geometry to conduct several transient, two-dimensional (2D) analyses for different materials. The software used to create the models was Structural Dynamics Research Corporation (SDRC) Integrated Design and Analysis Software (I-DEAS®). I-DEAS® uses a finite volume formulation to model heat conduction with a general geometry. The one-dimensional (1D) numerical and analytical results for steel rod convective heating, presented by Guidos (1995), were used to validate the I-DEAS® software before the analyses were completed. The computational time for each material is

a matter of minutes on a Silicon Graphics, Incorporated (SGI) 320 NT with a single Pentium® processor.

The 2D axisymmetric model is described in Figure 6, along with the monitoring points. The unstructured mesh contains 5,261 quadrilateral elements and 4,989 nodes with a mesh refinement of 0.09 mm at the surface. An initial temperature of 25° C was prescribed for the entire model, with a constant heat sink temperature load of 25° C on the bottom of the geometry.

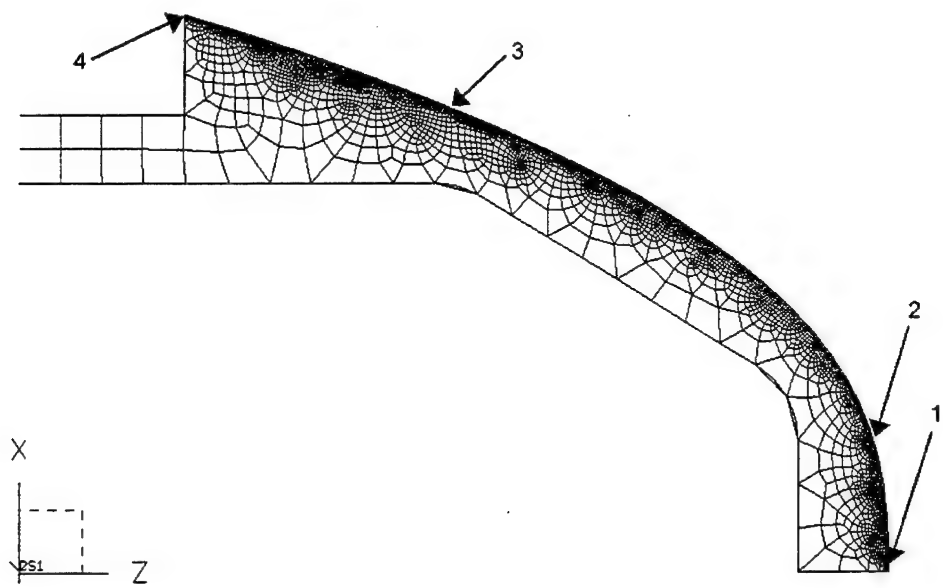

Figure 6. Axisymmetric Finite Element Mesh of General Radome Geometry.

I-DEAS® software is not capable of physical state changes such as melting. When the temperature of a monitoring point reached above the T_g or softening temperature, the material was declared inadequate for aero-heating. Material properties were also kept constant throughout the transient analysis.

4.2 Materials

Table 1 lists all the materials that were analyzed in this report. These materials were selected on the basis of a low dielectric constant, high heat capacity, and tensile strength.

4.3 Results

Using the various materials, the author computed temperatures for the radome geometry. Figures 7 through 12 show plots of the temperature history at monitoring points throughout the flight of the projectile. Figure 7 shows the temperature response of the radome if it were made of MACOR®. Since

MACOR® is capable of temperatures as great as 1000° C, the aerothermal heating was not considered a problem. However, the high dielectric constant disqualifies the material for use as a radome. Figure 8 depicts the temperature response of Ultem® 1000. Within a second, portions of the radome reach temperatures above the softening temperature and the T_g. Temperature response for Torlon® 4203 is displayed in Figure 9. Within 1.5 seconds, portions of the radome have temperatures that exceed both the softening and the T_g temperatures. Figure 10 shows the plots for 450GL30, 30% glass-reinforced PEEK®.

Table 1. Physical Properties of Studied Materials

	MACOR®	Nylon 66	Ultem®	Torlon® 4203	450GL30	Celazole®	Vespel®
Density (g/cc)	2.52	1.15	1.28	1.42	1.51	1.3	1.43
Young's modulus(Gpa)	66.9	2.9	3.3	4.0	6.89	6.2	2.4
Compressive strength (Mpa)	94	86	152	220	179	345	86.2
Poisson's ratio	.29	.4	.35	0.45	0.45	.3	0.41
Thermal conductivity (W/m/K)	1.46	.24	.13	0.26	.43	.4	.35
Softening temperature (°C)	N/A	93	200	278	232	427	360
Tg or melting (°C)	N/A	260	215	275	340	399	N/A
Specific heat (KJ/kg/°C)	.79	1.67	1.67	0.36	1.65	1.65	1.13
Dielectric constant	6.03	3.6	3.15	3.9	3.7	3.2	3.55

Because the temperatures reached the softening temperature, quasi-static linear finite element structural analyses were conducted on the radomes made of Ultem®, Torlon® 4203, and 450GL30. One analysis was performed with 20,000 g's launching acceleration with the material temperature at room temperature. A second analysis was conducted at a time in flight when the softening temperature had been achieved at some of the monitor points. The material properties of the entire model were changed to those when the material properties soften. The boundary loads consisted of 60-psi static pressure over the geometry. This analysis indicated that the radome geometry would significantly deform, possibly placing the material into a nonlinear plastic region of stress and strain and possibly impacting aerodynamic performance.

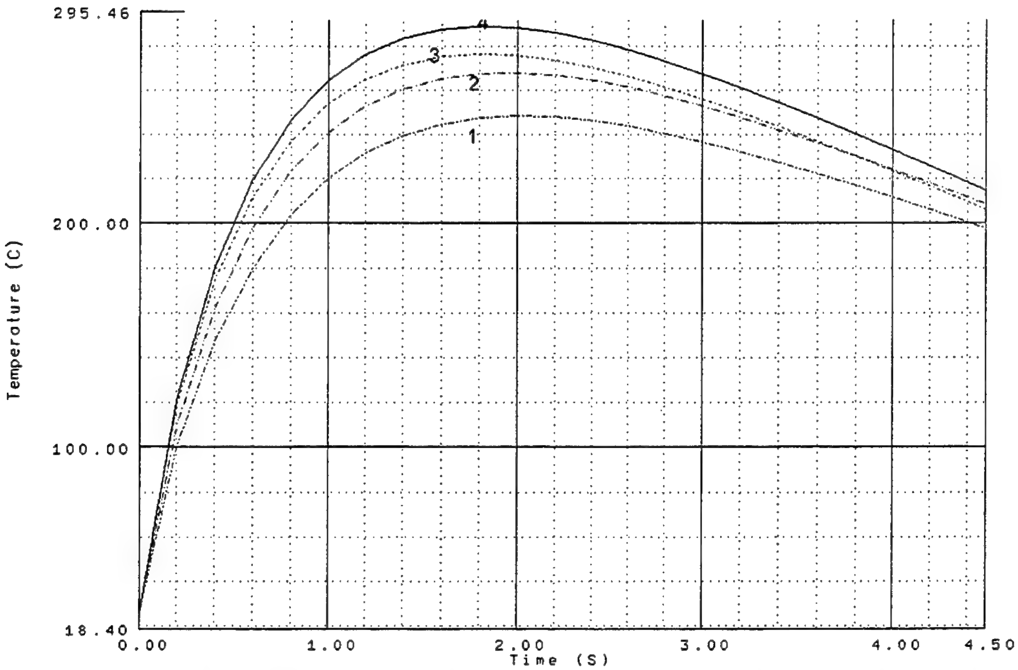

Figure 7. Computed Temperature Response at Radome Monitor Points for MACOR® With a Laminar to Turbulent Transition.

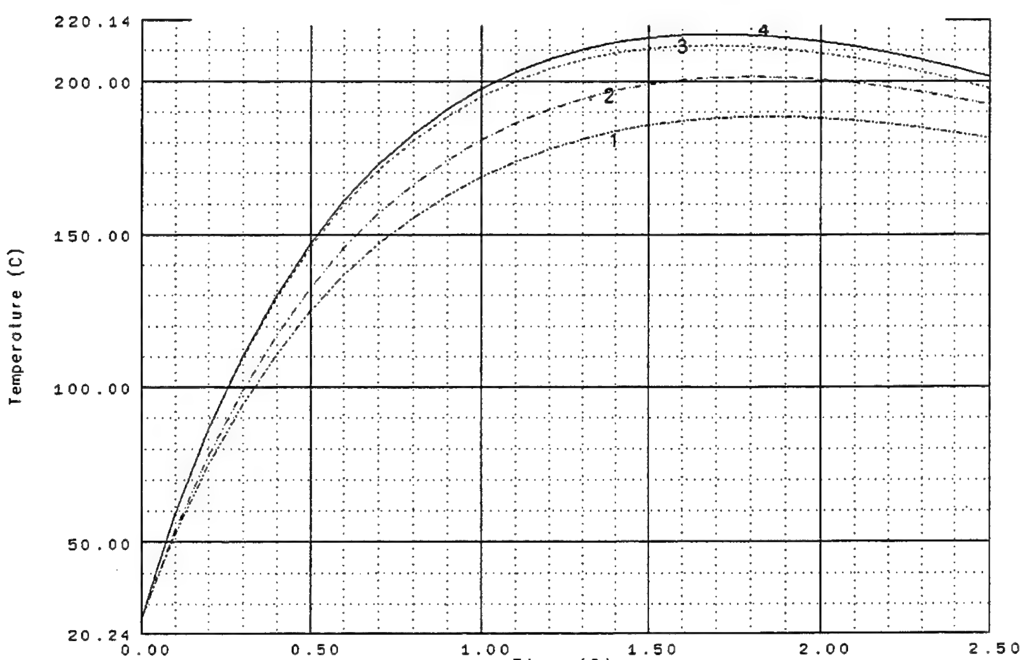

Figure 8. Computed Temperature Response at Radome Monitor Points for Ultem® 1000 With a Laminar to Turbulent Transition.

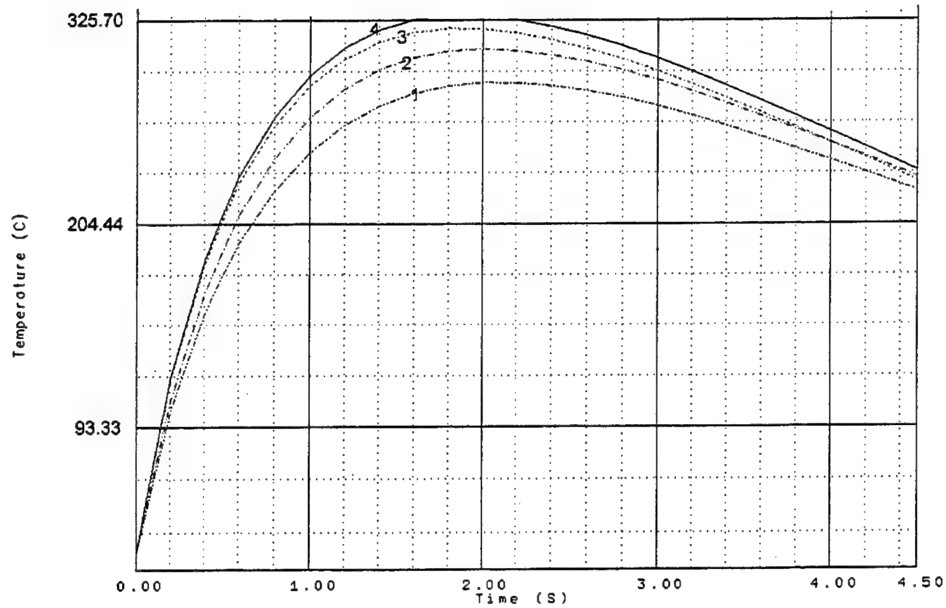

Figure 9. Computed Temperature Response at Radome Monitor Points for Torlon® 4203 With a Laminar to Turbulent Transition.

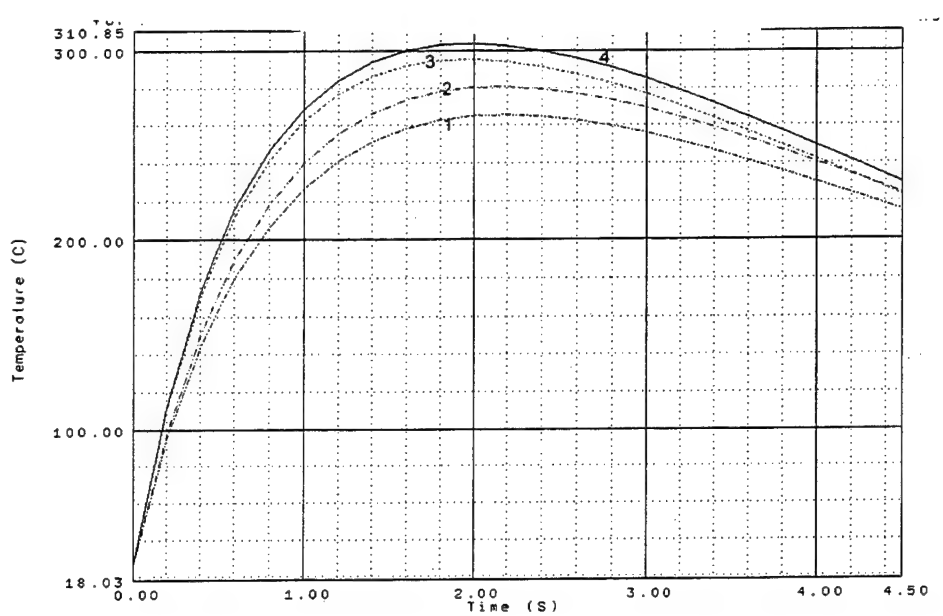

Figure 10. Computed Temperature Response at Radome Monitor Points for PEEK® 30% Glass Fiber Reinforced With a Laminar to Turbulent Transition.

Although this analysis is conservative, the 450GL30 was considered to be too weak at the higher temperatures for use. The computed temperature responses for Celazole® were very promising since the temperatures never exceeded the softening or the T_g temperatures. The temperature responses are displayed in Figure 11. Figure 12 displays the computed temperature responses of the monitoring points of a radome made from Vespel®. None of the temperatures reach the softening temperature; however, they do reach the T_g. Structural analyses indicated that the material would survive launching conditions and that the material structural properties did not decrease sufficiently to weaken the material during the supersonic flight profile. Nylon was not analyzed because of its low melting temperature.

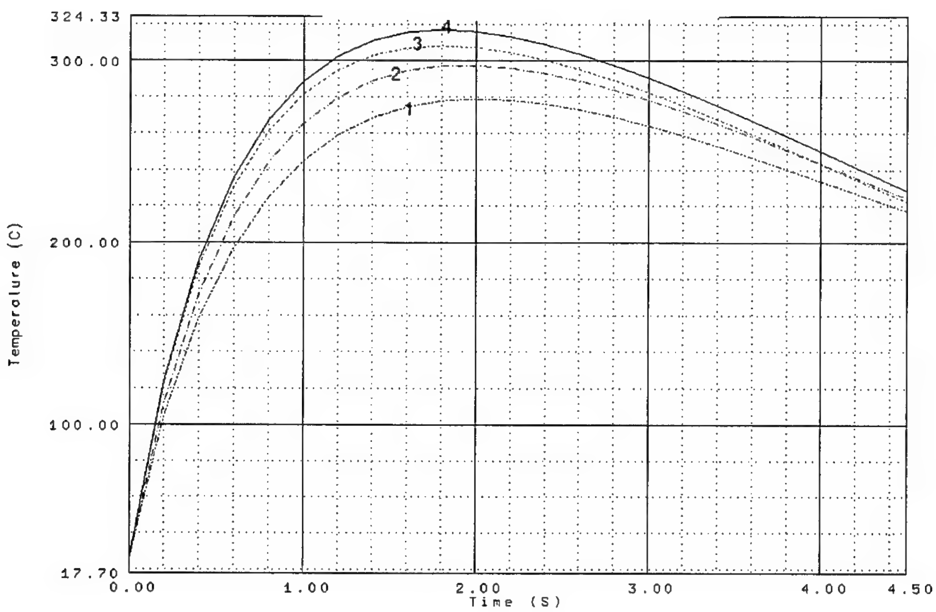

Figure 11. Computed Temperature Response at Radome Monitor Points for Celazole® With a Laminar to Turbulent Transition.

4.4 Model Verification

Analyses must be tempered with some data to validate the predictions. For the case of a yawsonde, flight experiences do exist, based upon flights conducted at Yuma Proving Ground (YPG), Arizona. A yawsonde was installed onto a modified M831 high explosive antitank tracer projectile (HEAT-TP), as seen in Figure 13. The projectile was launched at about 1060 m/s (M=3.1) and achieved a flight profile as seen in Figure 14. The projectile, with the large flat face immediately after the aerodynamic fuze body, decelerated quickly. This flight configuration survived the launch and flight, while telemetering data until it hit the desert floor. Although the aerothermal analysis had been conducted, the thermal analysis had never been performed. Instead, the yawsonde was designed with Nylon 66 because of its strength, thermal properties, and dielectric constant

(Hollis & Brandon 1999). To handle the high temperature stagnation region temperatures, however, the nylon windshield was fitted with a button screw made of MACOR®.

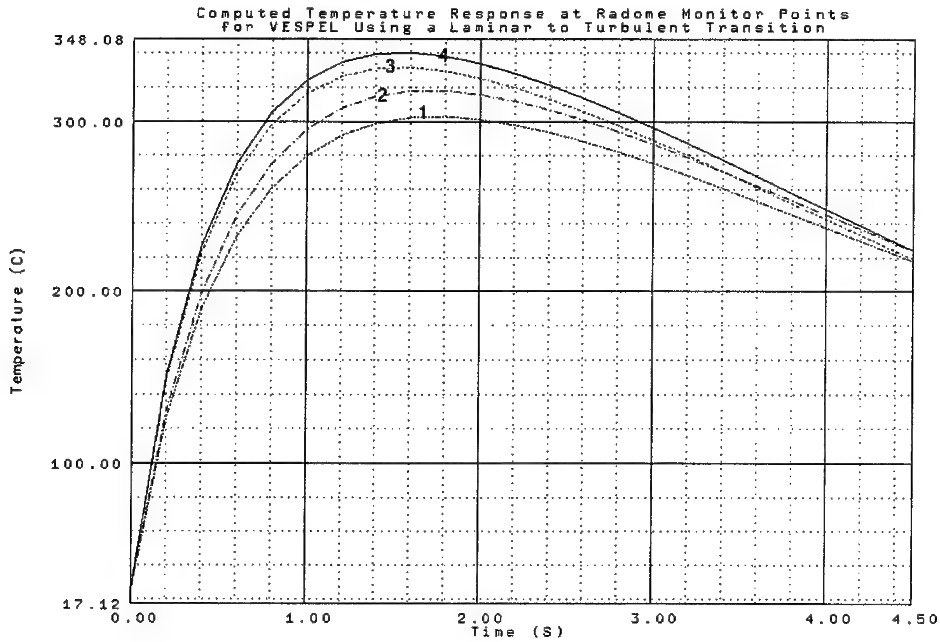

Figure 12. Computed Temperature Response at Radome Monitor Points for Vespel® With a Laminar to Turbulent Transition.

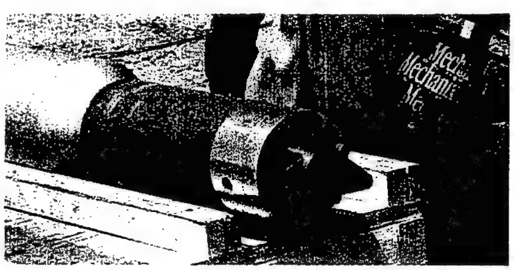

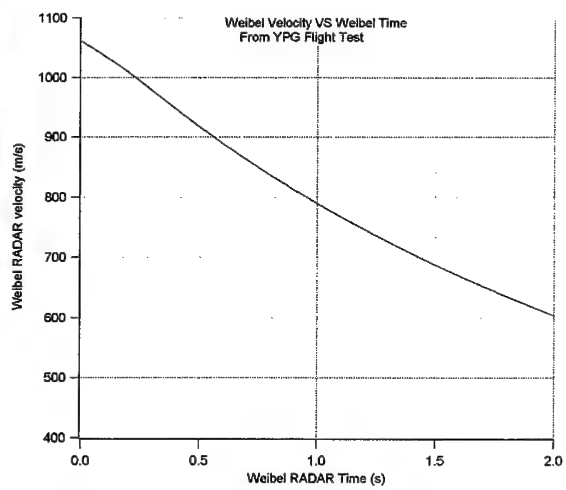

Figure 13. Yawsonde About to be Launched From a Gun on an M831 Projectile.

Figure 14. Weibel Velocity Versus Weibel Time From YPG Flight Test.

4.5 In-Flight Surface Heat Transfer

The aerodynamic heat transfer coefficient distributions were also obtained from separate analyses via ASCC. For validation of this report, an exterior axisymmetric geometry was modeled and solved for the initial part of the flight at the proper Mach numbers. Heat transfer coefficient, h, and the adiabatic wall temperature, T_{aw}, are the results of these models, acting along the geometry. Figures 15 and 16 show the laminar and turbulent heat transfer coefficients and T_{aw}, respectively. Also shown is a laminar-turbulent transition scheme for the heat transfer coefficients.

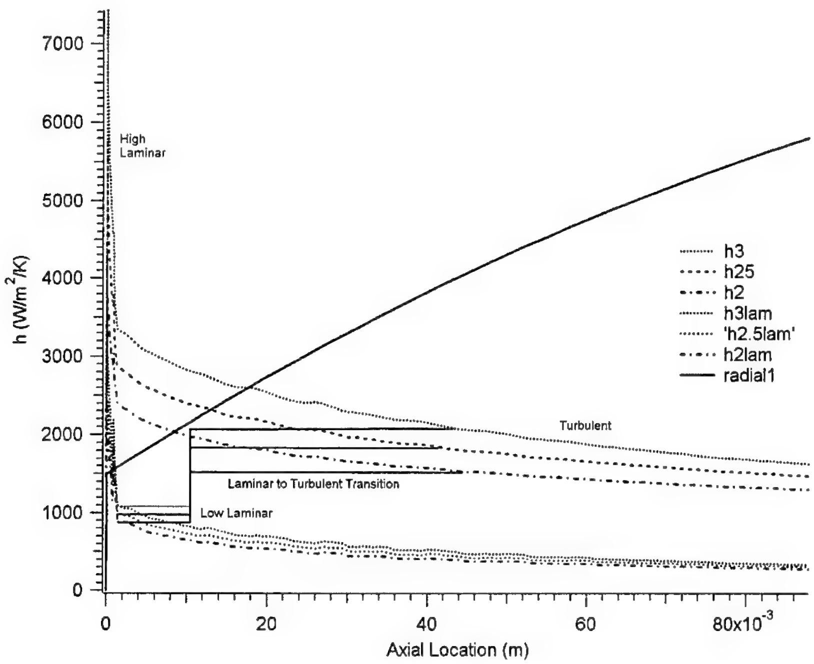

Figure 15. Comparison of Heat Transfer Coefficients at Various Mach Numbers for Turbulent and Laminar Flow Conditions for a Yawsonde.

4.6 In-depth Thermal Response of the Yawsonde

A 2D transient analysis was conducted for the multiple material yawsonde configuration. The analysis was also performed with the I-DEAS® code. The 2D geometry is described in Figure 17 with the transition points. The analysis used the laminar-to-turbulent boundary condition scheme developed with the ASCC. The multi-material model consists of aluminum, Stycast 1090-Si epoxy, which is used for encapsulating electronics, nylon 66, MACOR®, and air. Figure 18 displays the mesh and the monitor points: high heat transfer coefficient laminar(1), high-to-low heat transfer coefficient laminar(2), laminar-to-turbulent transition(3), monitor points 4 and 5, and a monitor point on the aluminum. Because of the differences in aerothermal heating between the hemispherical radome and the cone shape radome, the heat transfer coefficients were broken

into a few more regions for the cone shape. The mesh, which consists of 7,744 elements and 7,490 noses, is on the order of 0.14 mm in size near the surface of the yawsonde. Material properties used for the thermal analysis are displayed in Table 2. Nylon and MACOR® properties are given in Table 1.

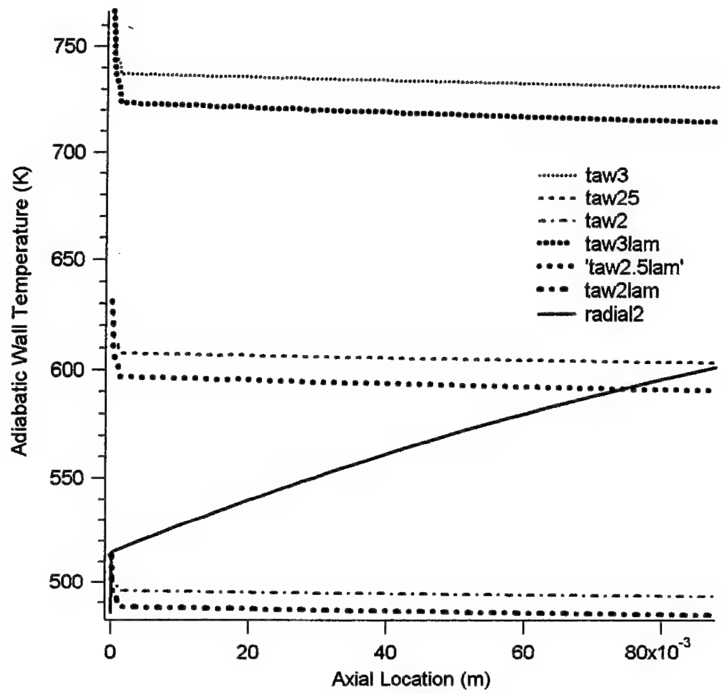

Figure 16. Steady State Adiabatic Wall Temperatures for Various Mach Numbers for the Yawsonde Geometry.

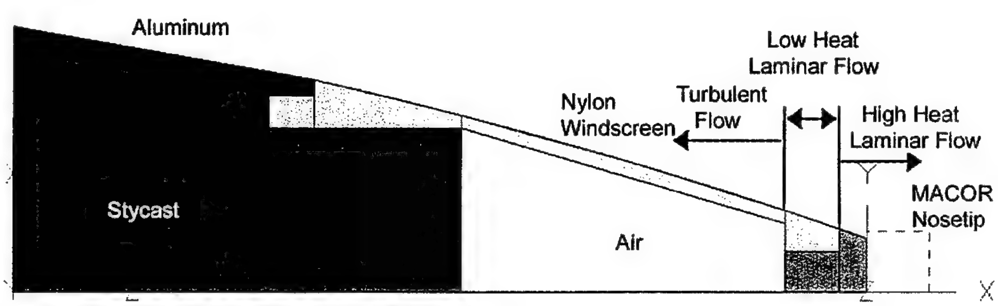

Figure 17. Axisymmetrical Layout of the Yawsonde Model.

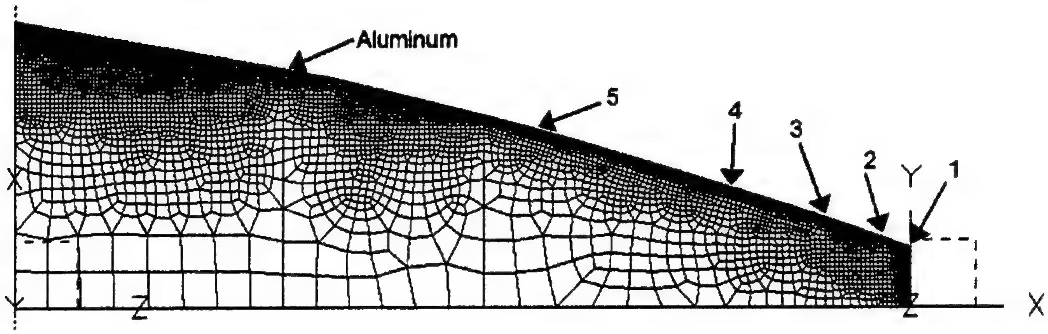

Figure 18. Axisymmetrical Finite Element Model of the Yawsonde.

Table 2. Material Properties Used for the Thermal Analysis

Material	ρ (g/cm³)	k(J/kg/K)	C_p (kJ/kg/K)
Aluminum	2.79	177.0	.875
Stycast 1090 SI	0.72	0.19	.385
Air (STP)	0.0013	26.3	1.007

5. Results

Figure 19 displays the temperature response for the laminar-to-turbulent flow scheme. Depicted are the temperature histories of the points from the previous figure. These temperature histories indicate that the windshield would survive the launch and flight. Since the yawsonde worked properly, even though the data report temperatures close to melting, one could assume that the analysis is quite conservative. A linear structural analysis with the material properties at room temperature was conducted and is discussed in Hollis and Brandon (1999).

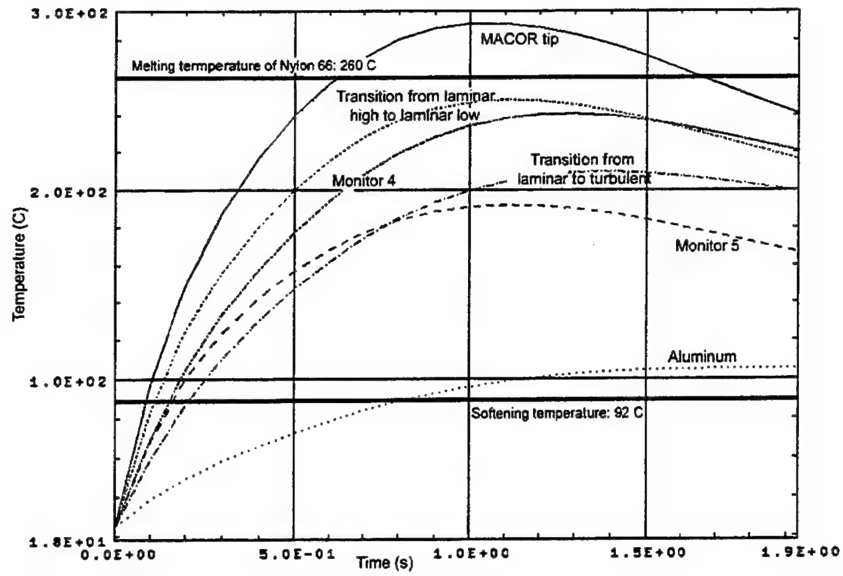

Figure 19. Computed Temperature Response of a Yawsonde With a Mach 3 Launch and a Laminar to Turbulent Transition Boundary Layer Scheme.

6. Conclusion

A series of transient thermal analyses with conservative input assumptions has been conducted on two different radome geometries. A gross indicator of "it worked" provides some validation of the predictions for the yawsonde radome and its materials, based upon flights at YPG. In this case, the laminar-to-turbulent flow scheme was used. Based on this method of analysis, one could choose from the previously mentioned polymers to manufacture a radome. The choices would be Celazole® or Vespel®. Since this analysis was performed to find a quick solution and since Celazole® is a specially ordered product not readily available, Vespel® is an appropriate choice for fabricating a radome because it is available in various extruded lengths.

7. Future Work

This report was aimed at finding a quick solution for a supersonic radome. The laminar-to-turbulent boundary condition imposed may not be accurate. During the revision phase of this report, the aerodynamic heat analyses were re-run for the hemispherical geometry and the yawsonde windshield. Inside the ASCC, a

switch was set for the computation to determine the transition point. This analysis yielded different results, which contained lower heat transfer coefficients than indicated in the imposed laminar-turbulent transition scheme. Future efforts should include refining the aerodynamic heat transfer analyses to improve accuracy.

In addition to suggesting a quick solution, it is also suggested that a more intensive effort be performed to find higher performance material solutions for the design of radomes for FCS-like projectile launch/flight conditions. The aerothermal, convective, conductive, and structural analyses are a skeleton of a study that needs to be performed. Materials that have functional temperatures in the region of the adiabatic wall temperatures of super and hypersonic vehicles need to be studied. Some of these materials may be ceramics, composites, and other polymers. Antenna radiation patterns and intensity measurements of the material and the geometry also need to be made. The structural analyses will need to be improved by implementing proper material orientation of the properties and by using LAMPAT[2] (Bogetti, Hoppel, & Burns 1995) for the composite materials. A linear solution for the structural analyses may be all that is necessary since the radome geometry should not deviate significantly so as not to affect aerodynamics. If the linear solution indicates nonlinear deformation, then the candidate material does not have sufficient strength.

[2] not an acronym

INTENTIONALLY LEFT BLANK

References

Acurex corporation/Aerotherm, "Aerotherm Assessment of Projectiles Using the ABRES Shape Change code (ASCC)," ARBRL-CR-00462, Ballistic Research Laboratory, Aberdeen Proving Ground, Maryland, August 1981.

Bogetti, T.A., C.P.R. Hoppel, and B.P. Burns, "LAMPAT: A Software Tool for Analyzing and Designing Thick Laminated Composite Structures," ARL-TR-890, U.S. Army Research Laboratory, Aberdeen Proving Ground, Maryland, September 1995.

Guidos, B.J., and W.B. Sturek, "Computation of Hypersonic Nosetip Heat Transfer Rates for an M829-Like Projectile," ARL-MR-52, U.S. Army Research Laboratory, Aberdeen Proving Ground, Maryland, April 1993.

Guidos, B.J., "Computed In-flight Temperature Response of a 120-mm XM797 Gas Generator Training Round Nose Cap," ARL-MR-267, U.S. Army Research Laboratory, Aberdeen Proving Ground, Maryland, October 1995.

Hepner, D.J., Muller, P.C., Hollis, M.S.L., Burke, L.W., D'Amico, W., Davis, B.S., Borgen, G., "An Aeroballistic Diagnostic Fuze," ARL Patent No. 00-44, U.S. Army Research Laboratory, Aberdeen Proving Ground, Maryland, patent pending.

Hollis, M.S.L., B.J. Guidos, and P.J. Conroy, "Thermal Analysis of a Subminiature Telemetry Sensor Mounted in a Kinetic Energy Projectile Base," ARL-TR-1425, U.S. Army Research Laboratory, Aberdeen Proving Ground, Maryland, August 1997.

Hollis, M.S.L., and F.J. Brandon, "Design and Analysis of a Fuze-Configurable Range Correction Device for an Artillery Projectile," ARL-TR-2074, U.S. Army Research Laboratory, Aberdeen Proving Ground, Maryland, December 1999.

Li, R., "Time-temperature Superposition Method for Glass Transition Temperature of Plastic Materials," Materials Science and Engineering A278 (2000), pp. 36-45, Elsevier, 1999.

INTENTIONALLY LEFT BLANK

Bibliography

Guidos, B.J., personal communications, U.S. Army Research Laboratory, Aberdeen Proving Ground, Maryland, May 2000.

McKnight, S., personal communications, U.S. Army Research Laboratory, Aberdeen Proving Ground, Maryland, June 2000.

Overfield, A., personal communications, DSM Engineering Plastic Products, Inc. Technical Group, Reading, Pennsylvania, June 2000.

Internet site, MatWeb, The Online Materials Information Resource, www.matweb.com.

Internet site, BP Amoco Chemicals-Engineering Polymers, www.bpamocaengpolymers.com.

Internet site, GE Plastics-Ultem 1000, www.geplastics.com.

Internet site, Accuratus Ceramic Corporation, MACOR, www.accuratus.com.

Internet site, DSM Engineering Plastic Products, www.dsmepp.matweb.com.

Internet site, www.Dupont.com/enggpolymers/Americas/vespel/docs/233630a.pdf.

INTENTIONALLY LEFT BLANK

NO. OF COPIES	ORGANIZATION
1	ADMINISTRATOR DEFENSE TECHNICAL INFO CTR ATTN DTIC OCA 8725 JOHN J KINGMAN RD STE 0944 FT BELVOIR VA 22060-6218
1	DIRECTOR US ARMY RSCH LABORATORY ATTN AMSRL CI AI R REC MGMT 2800 POWDER MILL RD ADELPHI MD 20783-1197
1	DIRECTOR US ARMY RSCH LABORATORY ATTN AMSRL CI LL TECH LIB 2800 POWDER MILL RD ADELPHI MD 20783-1197
1	DIRECTOR US ARMY RSCH LABORATORY ATTN AMSRL D D SMITH 2800 POWDER MILL RD ADELPHI MD 20783-1197
1	DIRECTOR US ARMY RSCH LABORATORY ATTN AMSRL SE RL B PIEKARSKI 2800 POWDER MILL RD ADELPHI MD 20783-1197
1	ARDEC ATTN AMSTA AR AEC T S LONGO PICATINNY ARSENAL NJ 07806-5000
4	ARDEC ATTN AMSTA AR AET A M AMORUSO D CARLUCCI S CHUNG R COLLET PICATINNY ARSENAL NJ 07806-5000
1	ARDEC ATTN AMSTA AR SCF D ATTN G ECKSTEIN PICATINNY ARSENAL NJ 07806-5000

NO. OF COPIES	ORGANIZATION
1	MCATD ARDEC ATTN NIGEL GRAY PICATINNY ARSENAL NJ 07806-5000
3	ARDEC ATTN AMSTA FSP A V ILLARDI R WERKO R SICIGNANO PICATINNY ARSENAL NJ 07806-5000
1	ADAWS ARDEC ATTN M MATTICE PICATINNY ARSENAL NJ 07806-5000
1	ARDEC ATTN W VOGT BLDG 171A PICATINNY ARSENAL NJ 07806-5000
1	ARDEC ATTN AMSTA AR FZ L SPRINGER PICATINNY ARSENAL NJ 07806-5000
3	REDSTONE TECHNICAL TEST CTR ATTN STERT TE F TD R EPPS S HAATAJA K WHIGHAM BLDG 7855 REDSTONE ARSENAL AL 35898-8052
1	AUBURN UNIVERSITY ATTN R BARRETT 211 AEROSPACE ENGINEER ST AUBURN UNIV AL 36849-5338
5	JOHNS HOPKINS APP PHYSICS LAB ATTN R BENSON H CHARLES JR R DENISSEN W DEVEREUX D WICKENDEN 11100 JOHN HOPKINS RD LAUREL MD 20723-6099

NO. OF COPIES	ORGANIZATION
1	MALLETT TECHNOLOGY ATTN M MAHELIC 14900 SWEITZER LN STE 202 LAUREL MD 20707-2915
1	BOLL SYSTEMS ASSOC ATTN R BODENSCHATZ 2001 N BEAUREGARD ST STE 800 ALEXANDRIA VA 22311-1772
2	IDA ATTN J FRASIER R SINGER 1801 N BEAUREGARD ST STE 800 ALEXANDRIA VA 22311-1772
1	DYN CORP ATTN B SNOWDEN 4001 FAIRFAX DR STE 200 ARLINGTON VA 22203
1	SRS TECHNOLOGIES ATTN J SUDDRETH 3900 FAIRFAX DR ARLINGTON VA 22203
1	DARPA ATTN B TANG 3701 FAIRFAX DR ARLINGTON VA 22203-1714
1	ALLIANT TECH INC ATTN J THALHEIMER 1911 N FT MEYER DR STE 800 ARLINGTON VA 22209
1	NATIONS INC ATTN R CARPENTER 12249 SCIENCE DRIVE ORLANDO FL 32826
3	STRICOM ATTN AMSTI LL R COLANGELO M PHILLIPS D SCHNEIDER 12350 RSCH PARK ORLANDO FL 32826-3276
1	NAWC ATTN WPNS G BORGEN 521 9TH ST BLDG 311 POINT MUGU CA 93042-5001

NO. OF COPIES	ORGANIZATION
2	NAWC ATTN L HOGE CODE 543E00E D POWELL CODE 543200E 521 9TH ST BLDG 311 POINT MUGU CA 93042-5001
1	NAWC ATTN S KUJIRAOKA 521 9TH ST BLDG 609 POINT MUGU CA 93042-5001
1	US ARO ENG & ENV SCIENCES DIV ATTN T DOLIGALSKI POB 12211 RSCH TRIANGLE PK NC 27709
2	AEROVIRONMENT INC ATTN A ANDRIUKOV M KEENNON 4685 3H INDUSTRIAL ST SIMI VALLEY CA 93063
1	ALLIANT TECHSYSTEMS ATTN C CANDLAND 600 SECOND STREET NE HOPKINS MN 55343-8384
2	KOI PRECISION PRODUCTS ATTN M CONE W KURTZ 3975 MCMANN ROAD CINCINATTI OH 45245-2395
1	R CHRISTIANSEN 3370 MIRALOMA AVE ANAHEIM CA 92803-3105
1	CREATIVE OPTICS ATTN J EBERSOLE 360 STATE ROUTE 101 BEDFORD NH 03110-5031
2	DRAPER LABORATORY ATTN J ELWELL J SITOMER 555 TECHNOLOGY SQ CAMBRIDGE MA 02139
1	ANALOG DEVICES ATTN B SULOUFF 21 OSBORN STREET CAMBRIDGE MA 02139-3556

NO. OF
COPIES ORGANIZATION

2 NAWC
ATTN S GATTIS CODE 54A000D
S MEYER CODE 543400D
1 ADMINISTRATION CIRCLE
CHINA LAKE CA 93555-6001

2 HAIGH-FARR
ATTN D FARR H FARR
12 INDUSTRIAL WAY
SALEM NH 03079

1 PATUXENT RIVER NAS
ATTN R FAULSTICH
UNIT 1 47765 RANCH RD
PAX RIVER MD 20670-1469

2 NSWC/DD
ATTN J FRAYSSE
D HAGAN CODE G304
17320 DAHLGREN ROAD
DAHLGREN VA 22448-5100

1 NSWC/IHDIV
ATTN D GARVICK CODE 40D
101 STRAUSS AVE
INDIAN HEAD MD 20640-5035

1 TOMMY HICKS
8816 CROSSWIND DRIVE
FORT WORTH TX 76719

1 GARY LEE
13627 PORTOFINO DRIVE
DEL MAR CA 92014

1 MACROVISION
ATTN T MACDONALD
55 WALKER'S BROOK DR
READING MA 01867-3297

1 ROBERT MEISENHELDER
804 WOBURN ST
WILMINGTON MA 01887-3462

1 ROBERT MIRACKI
3500 WEST BALCONES CTR
AUSTIN TX 78759-5398

1 WL/MNAV
ATTN G WINCHENBACH
101 W EGLIN BLVD
EGLIN AFB FL 32542-6810

NO. OF
COPIES ORGANIZATION

1 DAVID PAREKH
7220 RICHARDSON RD
SMYRNA GA 30080

2 PRIMEX TECHNOLOGIES
ATTN J BUZZETT
R TADDEO
10101 9TH STREET NORTH
ST PETERSBURG FL 33716

3 ARROW TECH ASSOC
ATTN W HATHAWAY
J WHYTE R WHYTE
1233 SHELBURNE RD
SOUTH BURLINGTON VT 05403

1 INTERSECT TECHNOLOGIES INC
ATTN GEORGE BALL
2030 E BROADWAY STE 215
TUCSON AZ 85719

1 SUKAMAR CHAKRAVARTHY
650 HAMPSHIRE ROAD
WESTLAKE VILLAGE CA
91361-2501

ABERDEEN PROVING GROUND

2 DIRECTOR
US ARMY RSCH LABORATORY
ATTN AMSRL CI LP (TECH LIB)
BLDG 305 APG AA

2 DIR ATC
ATTN STEAC TC E K MCMULLEN
H CUNNINGHAM
BLDG 400
APG AA

8 DIRECTOR
US ARMY RSCH LABORATORY
ATTN AMSRL WM BC P PLOSTINS
M BUNDY D LYON
B GUIDOS T ERLINE
J SAHU D WEBB
P WEINACHT
BLDG 390

NO. OF COPIES	ORGANIZATION
27	DIRECTOR US ARMY RSCH LABORATORY ATTN AMSRL WM BA T BROWN F BRANDON T BROSSEAU L BURKE W CLAY J CONDON B DAVIS J FAUST R HADDOX T HARKINS C HENRY D HEPNER M HOLLIS (5CYS) G KATULKA V LEITZKE R MCGEE J MCLAUGHLIN C MERMEGAN P MULLER P PERIGINO A THOMPSON S WANSACK R WERT BLDG 4600
1	DIRECTOR US ARMY RSCH LABORATORY ATTN AMSRL WM MA S MCKNIGHT BLDG 4600
5	DIRECTOR US ARMY RSCH LABORATORY ATTN AMSRL WM MB J BENDER T BOGETTI L BURTON B KASTE W SPURGEON BLDG 4600
4	DIRECTOR US ARMY RSCH LABORATORY ATTN AMSRL WM MC P HUANG J LASALVIA P PATEL J SWAB BLDG 4600

NO. OF COPIES	ORGANIZATION
2	DEFENCE EVAL & RSCH AGENCY ATTN R BEATTIE C CROMPTON DRA FORT HALSTEAD SEVENOAKS KENT TN14 7BP ENGLAND

INTENTIONALLY LEFT BLANK

REPORT DOCUMENTATION PAGE

Form Approved OMB No. 0704-0188

1. AGENCY USE ONLY *(Leave blank)*	2. REPORT DATE	3. REPORT TYPE AND DATES COVERED
	April 2001	Final

4. TITLE AND SUBTITLE

Parameterized Design of a Supersonic Radome

5. FUNDING NUMBERS

PR: AH80

6. AUTHOR(S)

Hollis, M.S.L. (ARL)

7. PERFORMING ORGANIZATION NAME(S) AND ADDRESS(ES)

U.S. Army Research Laboratory
Weapons & Materials Research Directorate
Aberdeen Proving Ground, MD 21005-5066

8. PERFORMING ORGANIZATION REPORT NUMBER

9. SPONSORING/MONITORING AGENCY NAME(S) AND ADDRESS(ES)

U.S. Army Research Laboratory
Weapons & Materials Research Directorate
Aberdeen Proving Ground, MD 21005-5066

10. SPONSORING/MONITORING AGENCY REPORT NUMBER

ARL-TR-2418

11. SUPPLEMENTARY NOTES

12a. DISTRIBUTION/AVAILABILITY STATEMENT

Approved for public release; distribution is unlimited.

12b. DISTRIBUTION CODE

13. ABSTRACT *(Maximum 200 words)*

With the new requirements of the future combat systems (FCS), gun-launched projectiles will most likely be decreasing in diameter and increasing in muzzle velocity. In addition, these projectiles will be carrying entire electronic systems, specifically, global positioning system (GPS)/inertial guidance and terminal homing. These systems will sense during the flight and terminal environments of the projectile and will provide data links (probably two-way telemetry) for system diagnostics and dynamic re-targeting. Most of these sensing elements involve various antennae operating at a variety of frequencies ranging from GPS (1.5 GHz) to millimeter wave seekers (94 GHz) to optical seekers (1 PHz). Because of packaging constraints, these systems are likely to be placed forward on the projectile body. All these antennae require a protective "window" for transmitting and/or receiving signals. Based on the location of these systems, that window is usually described as the projectile radome.

The radome must withstand the cannon launch and ballistic environment. The intense aero-heating of supersonic flight softens polymers, thus reducing the structural integrity. Of course, it is obvious that the radome must perform well electronically across a possible wide band of radio frequencies.

This report studies the use of several (polymer types) materials, which can be machined to create a radome of a desired shape. These polymers, which are either extruded or molded into stock shapes, were chosen based on the dielectric constant (relative to air, between 3 and 4) and thermal and structural properties. A generic radome geometry was selected to perform the thermal and structural analyses. An older yawsonde geometry, which was flight tested, was also analyzed.

In addition to suggesting a quick solution, it is also suggested that a more intensive effort be performed to find higher performance material solutions for the design of radomes for FCS-like projectile launch/flight conditions. The aerothermal, convective, conductive and structural analyses are a skeleton of a study that needs to be performed. Other materials such as ceramics, composites, and other polymers also need to be studied.

14. SUBJECT TERMS

microwaves, radio waves, thermophysical properties, polymers, thermal analysis

15. NUMBER OF PAGES

35

16. PRICE CODE

17. SECURITY CLASSIFICATION OF REPORT	18. SECURITY CLASSIFICATION OF THIS PAGE	19. SECURITY CLASSIFICATION OF ABSTRACT	20. LIMITATION OF ABSTRACT
Unclassified	Unclassified	Unclassified	